

# Uniform NE-SW Compression in the Devonian Grosmont Formation in NE Alberta: Constraints on Stress Directions and Magnitudes from Analysis of Drilling Induced Tensile Fractures

*Thomas Niederhuber  
Karlsruhe Institute of Technology*

*Micah Morin*

*Jason Nycz  
HELLAS 470 - Geophysics World Wide*

*Douglas R. Schmitt  
Purdue University*

*Birgit Müller  
Karlsruhe Institute of Technology*

## Summary

Hundreds of thousands of boreholes have been drilled within the Western Canada Sedimentary Basin; and the stress field in Alberta has been the subject of numerous studies. However, most of these are focused in deeper boreholes concentrated in the west near the front of the deformation zone, and there is little publicly available data in the NE portions of the basin. Here we use a combined approach of interpretation of tectonic information with results from Breakouts (BO) and Drilling Induced Tensile Fractures (DITFs) analysis to quantitatively constrain the principal stress magnitudes within the Devonian Grosmont Formation. High-resolution electrical image logs from 32 wells were evaluated for drilling-induced fractures and display a remarkable consistency in the stress directions of  $N41.8 \pm 16.5^\circ$ . By combining rock properties and geomechanical limitations with other logs, it was possible to subsequently delineate possible stress magnitudes to describe the complete stress field.

## Material and methods

The stress field in the Western Canadian Sedimentary Basin has been the subject of numerous studies (Bell & Gough, 1979; Fordjor et al., 1983; Adams and Bell, 1991; Shen et al 2019 and Wang et al 2023 in prep). As a result, many stress orientations have been collected over several decades (Reiter et al., 2014). The maximum horizontal compression orientation in Alberta is generally described as SW-NE (Bell and Gough 1979). Much of this data has been incorporated into the World Stress Map (WSM), a global stress database (Heidbach et al. 2018). However,

stress magnitude data are not consistently or publicly available for all regions of the Basin. The most comprehensive compilation was made by Bell and Grasby in 2012. It forms the basis for other analyses, such as that of Reiter and Heidbach (2014). For the area of investigation, they suggest a strike-slip tectonic regime, where  $S_{hmin} < S_V < S_{Hmax}$ .

Overall, however, there are few publicly available measurements of even stress direction indicators let along magnitudes in the northeastern part of the Basin. Interpretations rely heavily on interpolated stress directions (e.g. Reiter et al, 2014) representations are often used to describe the stress state, and these are necessarily associated with large uncertainties. This study seeks to provide additional information on both stress directions and magnitudes from the analysis of 32 image logs acquired over a Therefore, this study examined image logs from 32 wells drilled within a relatively small area (12.5km X 10 km) through the Grosmont Formation as part of evaluation studies for the Saleski Grosmont pilot project. Here we focus on technical aspects of the methodology to constrain stress magnitudes, and readers more interested in the geology of Grosmont Formation can find reviews in Arkadani et al (2014). The work here updates and extends the preliminary analysis of Morin 2017) but focusses on the technical aspects of stress constraint.

### Stress Orientation

Analyses of the directions of Drilling-Induced Tensile Fractures (DITFs) and Breakouts (BOs) are generally accepted to be one of the most reliable ways to indicate the orientations of the horizontal principal stresses in the crust (Schmitt et al, 2012). These form due to concentrations of the in situ stresses by the borehole cavity. Assuming a vertical borehole and that the vertical stress is a principal stress, tensile fractures will first form at the azimuth  $\phi$  of the maximum horizontal principal stress  $S_{Hmax}$  (Hubbert et al. 1957). In contrast, breakouts may form perpendicular to  $\phi$ . Ideally, both DITFs and BOs occur in pairs at 180° offset. These features are described many times in the literature and readers can find more details in Heidbach et al. (2016).

Image logs provide the ideal basis for such an evaluation because they can resolve both DITFs and BOs. Other techniques such as 4-arm calipers are often not suitable for this purpose. For this study, image logs from Weatherford HMI (High Resolution MicroImager) and Schlumberger FMI (Fullbore Formation MicroImager) are available. These were analyzed using the software StressFeatureAnalysis, which was developed using Matlab® (Fig. 1)

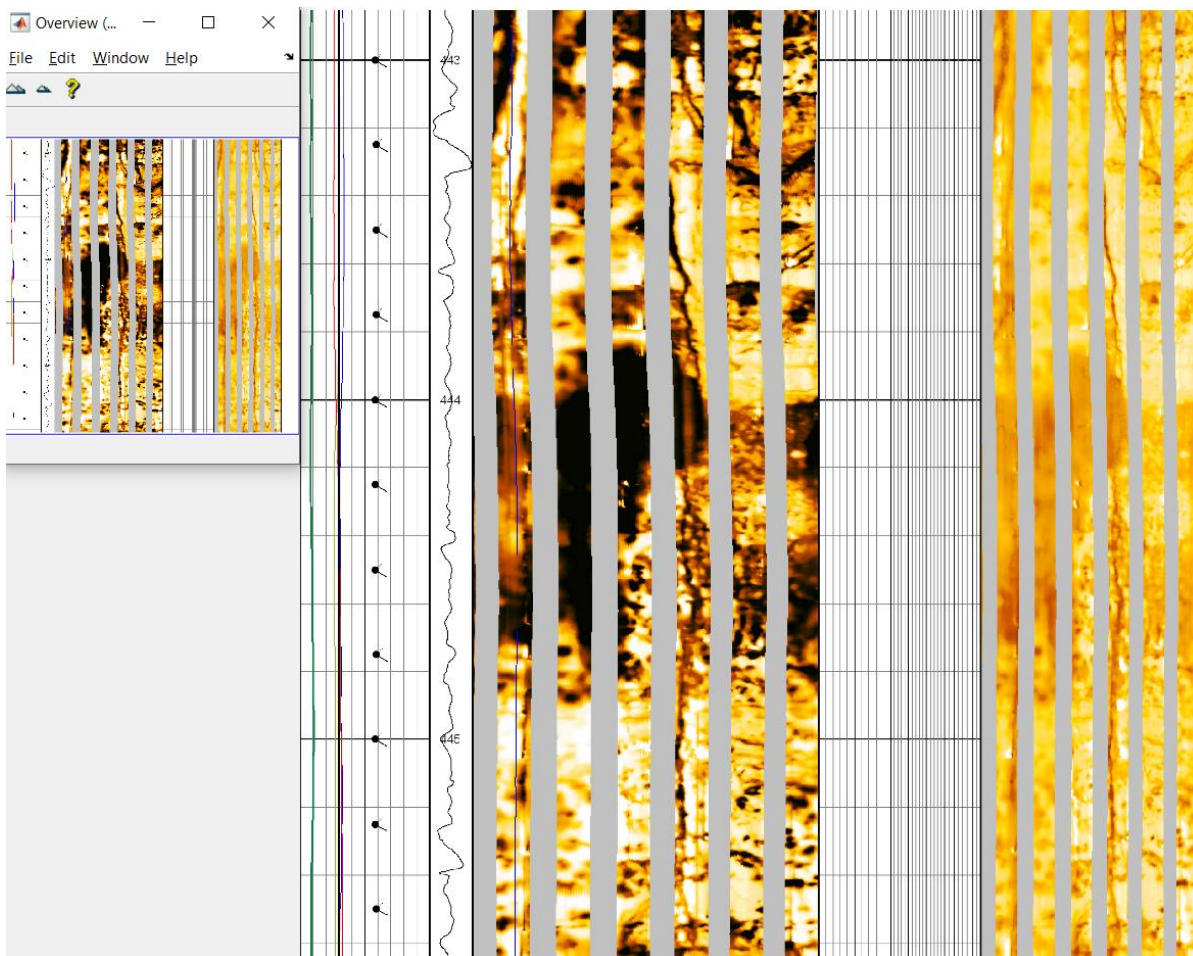


Fig. 2: Example from the StressFeatureAnalysis software. On the left is the dynamic and on the right the static HMI image with well-defined DITFs.

It is important to note that BO were observed, but DITF are nearly ubiquitous; the analyses below employ both the dearth of BO and the pervasive DITF's to constrain stress magnitudes.

First, the linear DITF were traced over 0.5m sections. This technique was chosen because many of the borehole logs have only few but very long DITFs. By using this method single outliers, which can be traced back to erroneous picking, can be eliminated. Afterwards, the results were processed using the bi-directional statistics of Mardia (1972) and categorized by the WSM ranking scheme (Heidbach et al. 2016).

In order to show spatial trends within the study area, gridded stress maps were created using the stress2grid software (Ziegler und Heidbach 2017). The software was adapted so that the search algorithm minimizes the standard deviation for each grid point. This method was chosen because, due to the small deviations in the stress direction, all grid points would otherwise be assigned the same value, since the termination criterion for extending the search radius would never be reached. With the new method local heterogeneities are shown on a very high level (WSM criteria better than quality C).

## Stress Magnitude

The pore pressure is an important quantity that is necessary in order to properly quantitatively describe the stress state as it will affect the value of many in situ physical properties and the points at which rocks fail or faults slip. As such, the pore pressure will influence the level at which BO or DITF initiate and to be able to constrain the total stress magnitudes it must be included. Pore pressure can be estimated by different transient pressure well tests.

Here we use values given by drill stem tests, as was done on two boreholes at different depths. The fluid mud pressure, was calculated based on mud densities which were given for each well. It represents the upper limit for the pore pressure and the lower limit for the minimum principal stress.

Vertical stress  $S_V$  was calculated by integrating the density logs from 22 wells. The minimum horizontal principal stress  $S_{hmin}$  is usually determined by hydraulic tests but these data do not exist at the site. Consequently, we instead constrain the horizontal stress magnitudes on the basis of the existence of the DITF.

As already noted, no BO are observed while extensive DITF's are found. Therefore, geomechanical conditions must exist that allow the formation of DITFs but not BOs. Due to the shallow depth of the boreholes, we assume that the thermal effects are small, so the thermal stress can be neglected. If only the borehole wall is considered, then for a vertical borehole in a strike slip tectonic regime where the vertical stress is the intermediate stress, the following applies (Moos und Zoback 1990):

$$\sigma_{rr} = \Delta P$$

$$\sigma_{\theta\theta}^{min} = 3S_{hmin} - S_{Hmax} - \Delta P - 2P_0$$

Where  $\sigma_{rr}$  is the radial stress,  $\sigma_{\theta\theta}$  is tangential stress,  $P_0$  is pore pressure and  $\Delta P$  is the difference of pore pressure and mud pressure.

To form DITFs the azimuthal stress must exceed the rock's tensile limit  $T_0$  ( $\sigma_{\theta\theta}^{min} \leq -T_0$ ) (Aadnoy 1990). Another criterion is that BOs occur as a result of shear failure. Therefore:

$$3S_{Hmax} - S_{hmin} - \Delta P - 2P_0 \geq \frac{2C \cdot \cos(\phi)}{1 - \sin(\phi)} + \frac{1 + \sin(\phi)}{1 - \sin(\phi)} \Delta P$$

Because both  $S_{Hmax}$  and  $S_{hmin}$  are unknown, a parameter study was performed in which both parameters were varied. But also, the parameters tensile stress  $T_0$ , unconfined compressive stress UCS, mud pressure  $P_{mud}$ , friction angle  $\phi$  and cohesion  $C$  have uncertainties, they were also varied in the parameter study.

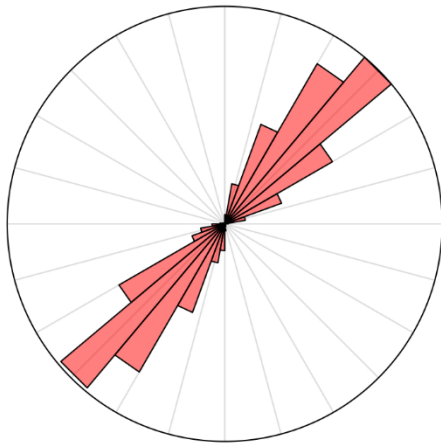
## Results and Discussion

### Stress Orientation

In the analysis of the 32 boreholes, a total of 1733 intervals were found to show DITFs. No breakout were identified. Approximately 3/4 of the total number of DITFs are associated with the Grosmont C formation.

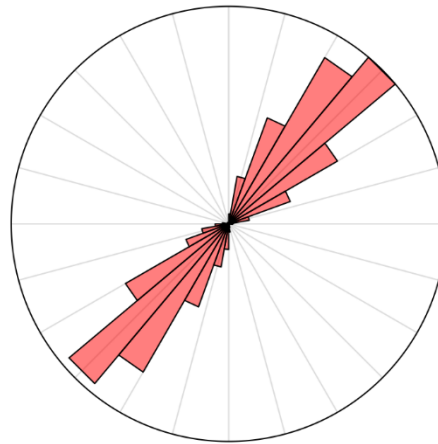
Using WSM criteria, 7 were classified as B, 5 as C, 19 as D and 1 as E. Using this as a basis, an average  $S_{Hmax}$  orientation of  $41.41^\circ \pm 16.26^\circ$  was calculated for all holes with a quality of A - C. If the D quality is also included, the average is  $41.55^\circ \pm 17.03^\circ$  (Fig. 2).

#### Quality A-C



$$\mu = 41.41^\circ \pm 16.26^\circ \quad R^2 = 0.85$$

#### Quality A-D



$$\mu = 41.55^\circ \pm 17.03^\circ \quad R^2 = 0.84$$

Fig. 2: Mean SH orientation calculated for all boreholes with quality A-C and for all boreholes with quality A-D according to the statistics of Mardia (1972).

For the analysis with stress2grid, in which the qualities as well as the relative distance to each other enter as a linear weighting function, this uniform stress pattern was confirmed (Fig. 3).

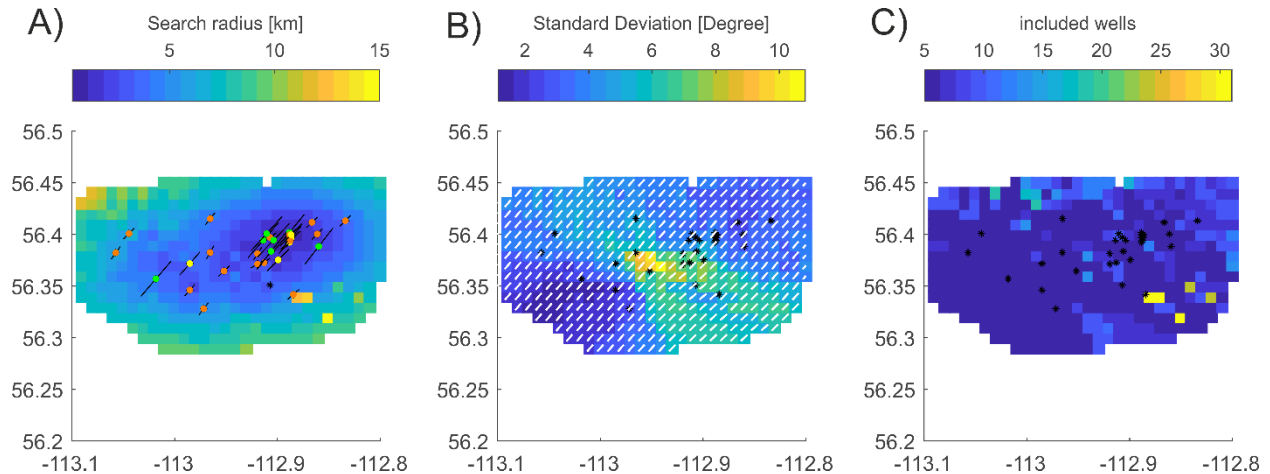


Fig.3: Results of the adapted Stress2Grid based on Ziegler and Heidbach (2017). Figure A shows the search radius used to determine the stress orientation, with large radius shown in yellow and small radius shown in blue. Holes were plotted as dots according to their WSM quality (green = B; yellow = C; orange = D). Figure B shows the standard deviation (yellow colors represent higher standard deviation while blue colors represent lower standard deviation) and the stress orientation as white lines. These are aligned with the stress orientation. Figure C shows how many holes are included the calculation of each cell average value.

NE-SW oriented stress field ( $N 42^\circ$ ) with a standard deviation of  $\leq 10\%$ . The maximum value occurs in the center of the field, while the lowest standard deviations were calculated for the northeastern part of the observed field. The search radius indicates the distance required to include the number of wells shown in Fig. 3 C, with a minimum of 5 wells. Due to the high density of wells with very similar stress orientations in the center, the search radius is very small, a few kilometers, while in the peripheral areas the search radius increases almost radially. The results confirmed the homogeneity of the stress field in this area, which had already been shown in previous studies for large areas of Alberta (Bell und Grasby 2012).

### Stress Magnitude

For the Grosmont Formation, pore pressures of 0.91 and 0.92 MPa are measured in 380 m depth. This corresponds to a pore pressure gradient of 2.39 and 2.42 MPa/km, respectively. Compared to the hydrostatic pressure with a gradient of 10 MPa/km, both measurements indicate significantly underpressured conditions that are consistent with issues encountered in drilling of this formation.

The vertical stress data for the strata above the Grosmont Formation is  $21.39 \text{ MPa/km} \pm 0.55 \text{ MPa/km}$ . Within the Grosmont Formation, the vertical stress gradient varies from 19.78 MPa/km to 27.02 MPa/km dependent on the density. The mean vertical stress gradient is 23.03 MPa/km with a standard deviation of 1.82 MPa/km.

As a result of the parameter study, the two horizontal stresses were determined at a depth of 380 m, the reference depth of the pore pressure measurement. The magnitude of the maximum horizontal stress  $S_{Hmax}$  reaches a value of 9.0 MPa. The minimum horizontal stress  $S_{Hmin}$  is 5.4

MPa. This corresponds to gradients of 23.7 MPa and 14.2 MPa respectively (Fig. 4). Thus, the maximum horizontal stress would be slightly greater than the vertical stress, resulting in a strike-slip tectonic regime according to Anderson (1905). This, as well as the magnitude of  $S_{hmin}$ , is also in agreement with previous studies such as Bell and Grasby (2012) and Morin (2017). The results are preliminary. They should be consolidated in further calculations and a range of error should be estimated.

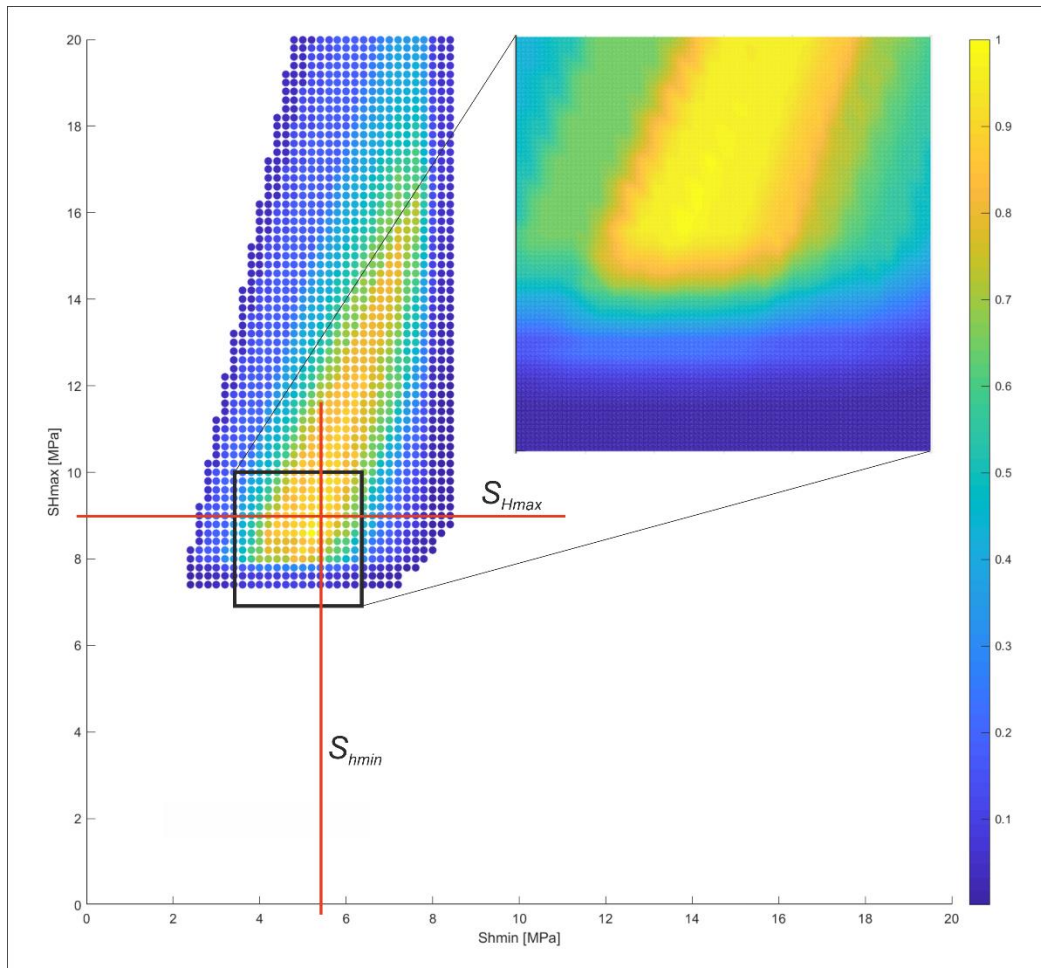


Fig.4: Results of the parameter study from which the two main horizontal stresses were derived. Shown in color are the possible combinations of  $S_{Hmax}$  and  $S_{hmin}$  that, under certain conditions, allow DITFs but not the formation of BO. The colors indicate the frequency with which each combination occurred. This value has been normalized to the maximum number, so that the maximum is one (yellow). The intersection of the two red lines shows the combination with the most events. Based on this, both magnitudes were estimated.

### Novel/Additive Information

These results are preliminary and may be subject to change as a result of further evaluation. However, what has already been shown is the surprisingly high number of DITFs. A stress state that allows them to form at a very shallow depth of a few hundred meters is rather surprising. This makes stress field characterization even more important for well integrity.

## Acknowledgements

I would like to thank all the authors involved for their cooperation. Special thanks to Micah Morin, who laid the foundation for this paper with his 2017 master's thesis.

## References

- Aadnoy, Bernt Sigve (1990): Inversion technique to determine the in-situ stress field from fracturing data. In: *Journal of Petroleum Science and Engineering* 4 (2), S. 127–141. DOI: 10.1016/0920-4105(90)90021-T
- Adams, J., Bell, J.S., 1991. Crustal stresses in Canada. *Neotectonics of North America* 1, 367–386.
- Bell, J. S.; Gough, D. I. (1979): Northeast-southwest compressive stress in Alberta evidence from oil wells. In: *Earth and Planetary Science Letters* 45 (2), S. 475–482. DOI: 10.1016/0012-821X(79)90146-8 .
- Bell, J. S.; Grasby, S. E. (2012): The stress regime of the Western Canadian sedimentary basin. In: *Geofluids* 12 (2), S. 150–165.
- Fordjor, C.K., Bell, J.S., Gough, D.I., 1983. Breakouts in Alberta and stress in the North American plate. *Can. J. Earth Sci.* 20 (9), 1445–1455.
- Heidbach, Oliver; Rajabi, Mojtaba; Cui, Xiaofeng; Fuchs, Karl; Müller, Birgit; Reinecker, John et al. (2018): The World Stress Map database release 2016: Crustal stress pattern across scales. In: *Tectonophysics* 744, S. 484–498. DOI: 10.1016/j.tecto.2018.07.007.
- Heidbach, Oliver; Rajabi, Mojtaba; Reiter, Karsten; Ziegler, Moritz; WSM Team (2016): World Stress Map Database Release 2016. Unter Mitarbeit von Oliver Heidbach, Mojtaba Rajabi, Karsten Reiter, Moritz Ziegler, WSM Team, J. Adams et al.
- Hubbert, M. King; Willis, David G.; others (1957): Mechanics Of Hydraulic Fracturing. In: *Petroleum Transactions, AIME* (210), S. 153–168.
- Mardia, K. V. (Hg.) (1972): *Statistics of directional data*. London: Academic Press (Probability and mathematical statistics, 13).
- Moos, Daniel; Zoback, Mark D. (1990): Utilization of observations of well bore failure to constrain the orientation and magnitude of crustal stresses: application to continental, Deep Sea Drilling Project, and Ocean Drilling Program boreholes. In: *J. Geophys. Res.* 95 (B6), S. 9305–9325.
- Morin, Micah L. (2017): Natural and drilling induced fractures in the Grosmont Formation, Alberta: implications for the state of stress. Masterthesis. University of Alberta. Department of Physics.
- Reiter, K., O. Heidbach, D.R. Schmitt, K. Haug, M. Ziegler, and I. Moeck, A revised crustal stress orientation database for Canada, *Tectonophysics*, 636, 111-124, doi: 10.1016/j.tecto.2014.08.006, 2014.
- Schmitt, D.R., C.A. Currie, and L. Zhang, Crustal stress determination from boreholes and rock cores: Fundamental principles, *Tectonophysics*, , doi:10.1016/j.tecto.2012.08.029, 580, 1-26, 2012.
- Shen, Luyi W.; Schmitt, Douglas R.; Haug, Kristine (2019): Quantitative constraints to the complete state of stress from the combined borehole and focal mechanism inversions: Fox Creek, Alberta. In: *Tectonophysics* 764, S. 110–123. DOI: 10.1016/j.tecto.2019.04.023.
- Terzaghi, Karl (1925): *Erdbaumechanik auf bodenphysikalischer Grundlage*. Mit 65 Textabb. Leipzig & Wien: F. Deuticke.
- Wang, Wenjing; Schmitt, Douglas Ray; Chan, Judith (2023): Heterogeneity versus Anisotropy and the State of Stress in Stable Cratons: Observations from a Deep Borehole of Opportunity in Northeastern Alberta, Canada. In: in press *J. Geophys. Res. Solid Earth*. DOI: 10.1002/essoar.10512083.1.
- Ziegler, Moritz; Heidbach, Oliver (2017): Matlab script Stress2Grid: GFZ Data Services.